View metadata, citation and similar papers at core.ac.uk

brought to you by CORE

provided by Xiamen University Institutional Repository

Molecular Biology of the Cell
Vol. 18, 4681–4689, November 2007

Adenine Nucleotide (ADP/ATP) Translocase 3 Participates in the Tumor Necrosis Factor–induced Apoptosis of MCF-7 Cells

Ziqiang Yang,* Wei Cheng,† Lixin Hong,† Wanze Chen,† Yanhai Wang,† Shengcai Lin,† Jiahuai Han,† Huamin Zhou,‡ and Jun Gu*

*National Laboratory of Protein Engineering and Plant Genetic Engineering, College of Life Sciences, Peking University, Beijing 100871, China; †The Key Laboratory of the Ministry of Education for Cell Biology and Tumor Cell Engineering, School of Life Sciences, Xiamen University, Xiamen, Fujian 361005, China; and ‡Department of Immunology, The Scripps Research Institute, La Jolla, CA 92037

Submitted December 29, 2006; Revised August 24, 2007; Accepted September 5, 2007
Monitoring Editor: John Cleveland

Mitochondrial adenine nucleotide translocase (ANT) is believed to be a component or a regulatory component of the mitochondrial permeability transition pore (mtPTP), which controls mitochondrial permeability transition during apoptosis. However, the role of ANT in apoptosis is still uncertain, because hepatocytes isolated from ANT knockout and wild-type mice are equally sensitive to TNF- and Fas-induced apoptosis. In a screen for genes required for tumor necrosis factor α (TNF-α)-induced apoptosis in MCF-7 human breast cancer cells using retrovirus insertion–mediated random mutagenesis, we discovered that the ANT3 gene is involved in TNF-α–induced cell death in MCF-7 cells. We further found that ANT3 is selectively required for TNF- and oxidative stress–induced cell death in MCF-7 cells, but it is dispensable for cell death induced by several other inducers. This data supplements previous data obtained from ANT knockout studies, indicating that ANT is involved in some apoptotic processes. We found that the resistance to TNF-α–induced apoptosis observed in ANT3 mutant ($ANT3^{mut}$) cells is associated with a deficiency in the regulation of the mitochondrial membrane potential and cytochrome c release. It is not related to intracellular ATP levels or survival pathways, supporting a previous model in which ANT regulates mtPTP. Our study provides genetic evidence supporting a role of ANT in apoptosis and suggests that the involvement of ANT in cell death is cell type– and stimulus-dependent.

INTRODUCTION

MCF-7 human breast cancer cells are widely utilized to study tumor necrosis factor α (TNF-α)-induced apoptosis. The apoptosis signaling in MCF-7 cells is initiated by TNF receptor I (TNF-RI) clustering that results from TNF and TNF-RI engagement. The clustered TNF-RI recruits the death domain (DD)-containing adapter protein TRADD (TNFRSF1A-associated via death domain) to their intracellular DDs. One function of TRADD is to bind to FADD (Fas-associating protein with death domain), which in turn stimulates caspase-8 autoactivation. Active caspase-8 is an initiator caspase that acts via cytochrome c (cyt c) release from the mitochondria to execute apoptosis in MCF-7 cells (Strasser *et al.*, 2000). TNF-α–induced reactive oxygen species (ROS) generation in mitochondria (Goossens *et al.*, 1995) is involved in apoptotic cell death and increases in mitochondrial membrane permeability transition (MPT) are believed to be essential in many apoptosis pathways (Pastorino *et al.*, 1996; Kroemer and Reed, 2000). The loss of inner mitochondrial membrane potential is associated with MPT and has been described as a common step in most apoptotic processes.

MPT is controlled by the mitochondrial permeability transition pore (mtPTP), which is believed to be formed by voltage-dependent anion channel (VDAC), members of the Bcl2 family, cyclophilin D, and adenine nucleotide (ADP/ATP) translocases (ANTs; Zamzami and Kroemer, 2001). The role of cyclophilin D in mtPTP has been confirmed by gene knockouts in mice (Baines *et al.*, 2005; Nakagawa *et al.*, 2005); however, the role of ANT remains controversial (Marzo *et al.*, 1998; Kokoszka *et al.*, 2004). Mitochondria from ANT knockout mouse livers still possess mtPTP activity, contradicting a widely accepted model for mtPTP (Kokoszka *et al.*, 2004). Moreover, sensitivity to TNF- and Fas-induced death is comparable in both ANT-deficient and wild-type hepatocytes (Kokoszka *et al.*, 2004). Nevertheless, the study did reveal using ANT-knockout hepatocytes that ANT has an essential role in modulating the sensitivity of mtPTP to Ca^{2+} activation and ANT ligands (Kokoszka *et al.*, 2004). Therefore, though ANT may not be an essential mtPTP structural component, the interaction of ANT with cyclophilin D and VDAC is still important in regulating mtPTP and perhaps is still required for apoptosis in some cell systems.

In humans there are four ANT isoforms sharing 60–80% identical sequences. ANT1, ANT2, and ANT4 are expressed in a tissue-specific manner, whereas ANT3 is ubiquitously expressed (Stepien *et al.*, 1992; Dolce *et al.*, 2005). Overex-

This article was published online ahead of print in *MBC in Press* (http://www.molbiolcell.org/cgi/doi/10.1091/mbc.E06–12–1161) on September 12, 2007.

Address correspondence to: Huamin Zhou (huaminzhou@xmu.edu.cn) or Jun Gu (gj@pku.edu.cn).

Abbreviations used: ANT, adenine nucleotide translocase; MPT, mitochondrial permeability transition; TNF, tumor necrosis factor.

© 2007 by The American Society for Cell Biology

pression of ANT1 or ANT3 has been reported to induce apoptosis with a concomitant decrease in mitochondrial inner membrane potential ($\Delta\Psi m$), whereas the overexpression of ANT2 had no effect on cell death (Bauer *et al.*, 1999; Zamora *et al.*, 2004). Apart from the potential role in MPT, ANT transports ADP and ATP across the mitochondrial inner membrane, which is essential for mitochondrial ATP synthesis and cytosol ATP supply. Interestingly, a recent study suggests that reducing ATP levels by inhibiting ANT enhances the necrotic process (Temkin *et al.*, 2006). It appears that ANT's role in both MPT and nucleotide translocation are directly or indirectly involved in cell death. However, genetic evidence for the requirement of ANT in apoptosis is still lacking. As for TNF-α–induced apoptosis, the role of ANT in cells other than hepatocytes has not been studied.

In search for genes that mediate apoptosis in TNF-α–treated MCF-7 cells, we used a random gene disruption approach to generate a series of MCF-7 mutants that are resistant to TNF-α–induced cell death (Ono *et al.*, 2001; Wang *et al.*, 2001; Zarubin *et al.*, 2005; da Silva *et al.*, 2006). The gene disrupted in one of the TNF-resistant lines was identified as ANT3. We show that hypomorphic expression of ANT3 in this mutant line is responsible for its low sensitivity to TNF-α–induced cell death, providing genetic evidence that ANT3 is required for the TNF-α–induced death of MCF-7 breast cancer cells. Our characterization of the ANT3-deficient MCF-7 cells suggests that ANT3 is involved in TNF-α–induced MPT and influences ROS production.

MATERIALS AND METHODS

Reagents

Recombinant human TNF was purchased from Promega (Madison, WI). zVAD-fmk was purchased from Calbiochem (La Jolla, CA). Cycloheximide (CHX), propidium iodide (PI), valinomycin, oligomycin, H_2O_2, and diquat dibromide (DQ) were purchased from Sigma (St. Louis, MO). DQ, instead of H_2O_2, was used in some of the studies of oxidation stress–induced cell death because it does not need to be freshly made every time. Hydroethidine (HE), DCFH-DA (2′,7′-dichlorofluorescin-diacetate), and JC-1 (5,5′,6,6′-tetrachloro-1,1′,3,3′-tetraethylbenzimidazolyl carbocyanine iodide) were purchased from Molecular Probes (Eugene, OR).

Retroviral Mutagenesis Screening

A clone of an MCF-7 cell, which exhibited a spontaneous survival rate of <1 in 10^6, was randomly mutated with the retrovirus pDisrup, selected with TNF, and analyzed by the 3′ rapid amplification of cDNA ends (RACE) technique as described previously (da Silva *et al.*, 2006). The endogenous gene that was fused with the *blasticidin*$^+$ gene was determined by DNA sequencing of the 3′RACE product. The primers used in the 3′RACE are as follows: primer room temperature (RT) 5′-CCA GTG AGC AGA GTG ACG AGG ACT CGA GCT CAA GC[T]$_{17}$-3′; nested PCR primers: P1/Q1 (5′-AAA GCG ATA GTG AAG GAC AGT GA-3′ and 5′-CCA GTG AGC AGA GTG ACG-3′) and P2/Q2 (5′-TGC TGC CCT CTG GTT ATG TGT GG-3′ and 5′-GAG GAC TCG AGC TCA AGC-3′). P1 and P2 are located on the *balsticidin*$^+$ gene, whereas Q1 and Q2 are on the anchor sequence of RT.

Constructs

cDNA of ANT3 was cloned into the KpnI and EcoRI sites of the vector pcDNA3 (Invitrogen, Carlsbad, CA), or it was cloned into the XbaI and XhoI sites of the vector pLenti. Annealed oligos for ANT2 and ANT3 RNA interference (RNAi) were cloned into the HpaI and XhoI sites of the vector pLentiLox3.7.

Cell Culture

Wild-type MCF-7 cells, ANT3^{mut} MCF-7 cells, and 293T cells were maintained in high-glucose DMEM (Invitrogen) supplemented with 10% newborn bovine serum, 100 U/ml penicillin, and 100 μg/ml streptomycin at 37°C and 5% CO_2 in a humidified incubator. In some experiments, cells were changed to glucose-free DMEM (Invitrogen) with 10% dialyzed newborn bovine serum.

Measurement of Cell Survival Rate

Cell survival rates were determined by flow cytometry with two parameters: plasma membrane integrity and cell size. The plasma membrane integrity was tested by the ability of cells to exclude PI. Cells were trypsinized, collected by centrifugation, washed once with phosphate-buffered saline (PBS), and resuspended in PBS containing 1 μg/ml PI. The levels of PI incorporation were quantified on a FACScan flow cytometer (EPICS XL; Beckman Coulter, Fullerton, CA). Cell size was evaluated by forward-angle light scattering. PI-negative cells with a normal size were considered living. The Annexin V-FITC kit (Roche Molecular Biochemicals, Indianapolis, IN) was used to measure PS flipping according to the manufacturer's protocol.

Measurement of ROS

ROS levels were determined by flow cytometry using the probes HE or DCFH-DA (Molecular Probes). HE is ready to be oxidized in the presence of ROS and gives a fluorescence emission that can be detected in the FL2 channel (575-nm filter). DCFH-DA, when inside in the cell, is cleaved by nonspecific esterase and releases carboxydichlorofluorescein. The released group is oxidized by ROS and gives a fluorescence emission that can be detected in the FL1 channel (525-nm filter). Cells were collected and washed once with PBS. The pellets were resuspended in PBS containing 6.6 μM HE or 10 μM DCFH-DA and 1 μg/ml PI, incubated for 45 min at 37°C. PI-negative cells were gated and analyzed by FL2 or FL1 channels, respectively.

Measurement of Mitochondrial $\Delta\Psi m$

Fluorescence microscopy or flow cytometry was used to analyze changes in $\Delta\Psi m$ with the probe JC-1 (Molecular Probes), as described in Ferguson *et al.* (2003), following the manufacturer's instruction. The cationic dye JC-1 can exist as a monomer or as JC-1 aggregates (J-aggregates), respectively, giving green and red fluorescence emissions. For flow cytometry, cells were collected and then washed once with PBS. The pellets were resuspended in normal medium containing 2.5 μg/ml JC-1. After being incubated for 30 min at 37°C and 5% CO_2, cells were washed twice with PBS and resuspended in PBS. Forward scattering (FSC) versus side scattering (SSC) was used to gate live cells for analysis of green (FL1, 525-nm filter) and red (FL2, 575-nm filter) fluorescence emissions on a FACScan flow cytometer (EPICS XL; Beckman Coulter). The cell population with a large FL2 value and small FL1 value was counted as the percentage of J-aggregate–positive cells. Because the K^+ ionophore valinomycin disrupts $\Delta\Psi m$, valinomycin (5 μg/ml)-treated cells were used as a standard for cells with disrupted $\Delta\Psi m$.

Measurement of ATP Levels

ATP was extracted by the boiling Method. Cells ($n = 4 \times 10^5$) were collected, washed once with PBS, resuspended in 100 μl boiling buffer (100 mM Tris, 4 mM EDTA, pH 7.75), and incubated at 100°C for 2 min. Samples were centrifuged at 10,000 $\times$ *g* for 60 s. ATP levels in the supernatants were determined using the ENLITEN ATP assay kit (Promega). Protein content was determined using the Coomassie brilliant blue G-250 assay kit. The ATP levels were normalized to protein content.

Cell Fractionation and Western Blot Analysis

Cell fractionation was performed mainly as described in Goldstein *et al.* (2000). Cells ($n = 2 \times 10^7$) were collected and washed once with ice-cold PBS. The pellets were resuspended in 1 ml ice-cold homogenization buffer (250 mM sucrose, 20 mM HEPES-KOH, pH 7.4, 10 mM KCl, 1.5 mM $MgCl_2$, 1 mM EDTA, 1 mM EGTA, 1 mM dithiothreitol [DTT], 1 mM phenylmethylsulfonyl fluoride [PMSF], and 10 μg/ml leupeptin). After sitting on ice for 15 min, the cells were disrupted by 200 strokes in a 1-ml Kontes douncer with the B-type pestle (Kontes Glass, Vineland, NJ). The nuclei were removed by centrifugation twice at 1000 $\times$ *g* for 10 min at 4°C. The supernatant was further centrifuged at 17,000 $\times$ *g* for 15 min. The resulting supernatant was the cytosol fraction and was used for Western blot (WB) analysis. For WB analysis, 30 μg of protein was resolved on a 15% SDS-polyacrylamide gel, transferred to a PVDF membrane, and then probed with anti-cyt c or anti-ANT antibodies (1:1000, Santa Cruz Biotechnology, Santa Cruz, CA) for 1 h at RT. After being incubated with horseradish peroxidase–conjugated secondary antibodies (1:2000) for 1 h at RT, the presence of a protein band was visualized using enhanced chemiluminescence (ECL) detection reagents (Amersham Pharmacia Biotech, Piscataway, NJ). The same membrane was stripped (three times using 2% SDS, 50 mM Tris, and 100 mM 2-mercaptoethanol for 20 min at RT and pH 6.5) and reprobed with anti-actin antibodies for 1 h at RT. The membrane was then incubated with secondary antibodies (1 h at RT) and visualized using the ECL system.

Virus Production and Infection

293T cells were used for virus production. Cells were plated in 10-cm dishes 18 h before transfection. The calcium phosphate precipitation method was used to transfect of 80% confluent cells with lentivirus vectors. Cells were changed to fresh medium 12 h later. The medium was collected 40 h later, filtered through a 0.45-μm filter, and centrifuged at 75,000 $\times$ *g* for 2 h at 4°C.

The virus pellets were resuspended in fresh medium containing 10 μg/ml polybrene for infection.

Measurement of mRNA Levels

Semiquantitative PCR was performed as described previously (Ono *et al.*, 2001). Forward and reverse primers for ANT1 PCR were as follows: 5′-CTGCCTACTTCGGAGTCTATG-3′ and 5′-CTTTCAGTCTGGTTTTATCCC-3′. Primers for ANT2 PCR were as follows: 5′-TCCCAAGAACACTCACATCG-3′ and 5′-ATGGAAATGGCTTTAGAGGA-3′. Primers for ANT3 PCR were as follows: 5′-GGGAAAGTCAGGCACAGAGCG-3′ and 5′-CGTACAGGACCAGCACGAAGG-3′. For real-time PCR analysis, 0.5 μg of total RNA was used to prepare cDNA using oligo$(dT)_{12}$ as a primer. The SYBR green PCR Master Mix kit (Applied Biosystems, Foster City, CA) was used for real-time PCR analysis.

RNAi

Vector-based RNAi was used to knock down ANT2 or ANT3 expression. For ANT2 RNAi, the target sequence was GTATCTATGACACTGCAAA; for ANT3, the target sequence was CACATCGTGGTGAGCTGGA.

Electrophoretic Mobility Shift Assay

Nuclear Protein Preparation. Cells (n = 2 × 10^6) in a 60-mm dish were washed once with PBS, scraped with 1 ml 2.5 mM EDTA-PBS solution and collected by centrifugation at 1500 × *g* for 5 min at 4°C. The cell pellets were resuspended in 160 μl of cold buffer A (10 mM HEPES, pH 7.9, 1.5 mM $MgCl_2$, 10 mM KCl, 1 mM DTT, 1 mM PMSF, and 10 μg/ml aprotinin) by gentle pipetting. The cells were allowed to swell on ice for 15 min, and then 40 μl of 2.5% NP-40 in buffer A was added and vigorously vortexed for 10 s. The nuclear pellets were collected by centrifugation at 1500 × *g* for 5 min at 4°C, resuspended in 40 μl of ice-cold buffer C (20 mM HEPES, pH 7.9, 0.4 M NaCl, 1 mM EDTA, 1 mM DTT, and 1 mM PMSF), vortexed for 25 min at 4°C, and then centrifuged at 15,000× *g* for 5 min at 4°C. The supernatant was frozen in aliquots at −70°C.

Gel Shift Assay. The probes were chemically synthesized, 3′ end biotin-labeled using the Biotin 3′ End DNA Labeling Kit (Pierce, Rockford, IL), and annealed following the manufacturer's instructions. Sense and antisense probe sequences for the nuclear factor-κB (NF-κB)-binding site were as follows: 5′-AGT TGA GGG GAC TTT CCC AGG C-3′ and 3′-TCA ACT CCC CTG AAA GGG TCC G-5′. EMSA was performed following the LightShift Chemiluminescent EMSA Kit instruction (Pierce). Briefly, 8 μg nuclear protein, 1 μg poly(dI:dC) were incubated in the reaction buffer containing 10 mM Tris (pH 7.5), 50 mM KCl, 5 mM $MgCl_2$, 1 mM DTT, 2.5% glycerol, and 0.05% NP40 for 10 min at RT, and then 50 fmol biotin-labeled probes were added and incubated for another 20 min at RT. After incubation, 2 μl loading buffer containing 0.3% bromophenol blue/3% glycerol was added. The mixtures were separated by electrophoresis through a nondenaturing 4% polyacrylamide gel. Then the binding complexes were transferred to a nylon membrane. Transferred DNA was cross-linked to membrane by UV. The biotin labeled DNA was detected by chemiluminescence.

Southern Blot Analysis

Genomic DNA from wild-type and ANT3^{mut} MCF-7 cells was digested with EcoRI and XmnI. The DNA fragments were resolved by 1% agarose gel electrophoresis, blotted onto a nitrocellulose membrane, and detected with a random-primed ^{32}P-labeled probe obtained using a DNA fragment containing exon 4 of human ANT3.

Statistical Analysis

Student's *t* test was used.

RESULTS

ANT3 Is Involved in the TNF-α–induced Apoptosis of MCF-7 Cells

Because the MCF-7 breast cancer epithelial cell line is frequently used as a model to study TNF-α–induced apoptosis, we used it to identify genes required for TNF-α–induced cell death by using a retroviral-induced mutagenesis approach (da Silva *et al.*, 2006). Retroviral integration can generate mutant alleles resulting in diminished or abolished expression of the target gene. Cells with mutations in genes required for TNF-α–induced killing may become TNF resistant and may be selected by TNF treatment. We selected a number of TNF resistance clones and determined that one of the resistant clones contained a disrupted *ANT3* gene; we termed this clone ANT3^{mut}.

Figure 1A shows that ANT3^{mut} cells are resistant to TNF-α–induced cell death unlike parental wild-type MCF-7 cells. The ANT3^{mut} cells are also resistant to TNF+CHX-induced cell death, though to a lesser extent (Figure 1B). The retroviral insertion in ANT3^{mut} cells was located 219 nucleotides

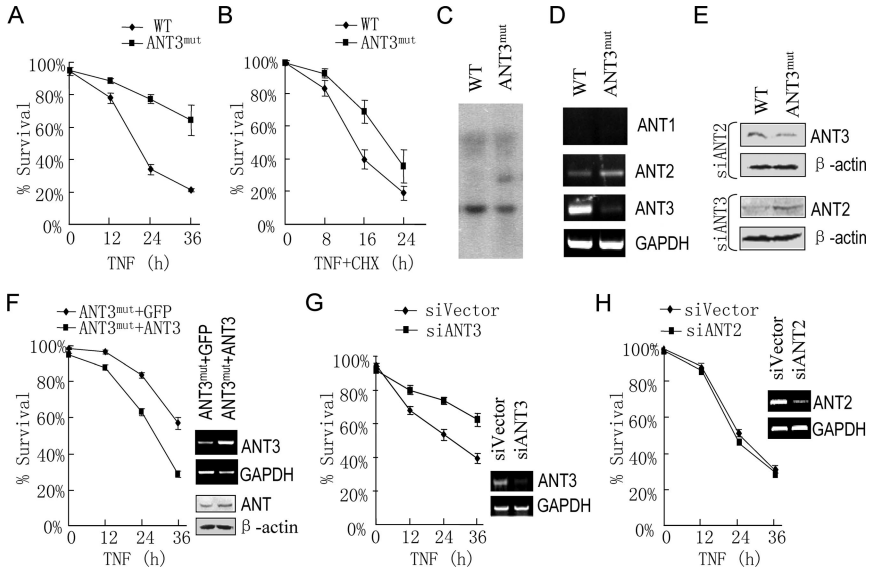

Figure 1. ANT3 mutation in MCF-7 cells led to a resistance to TNF-α–induced cell death. (A) Parental wild-type (WT) and ANT3^{mut} MCF-7 cells were treated with TNF-α (50 ng/ml) for different periods of time, and cell survival rates were measured by PI exclusion. (B) WT and ANT3^{mut} cells were treated with TNF-α (50 ng/ml) + CHX (1 μg/ml) for different periods of time, and cell survival rates were measured by PI exclusion. (C) Southern blot analysis of genomic DNA digested with EcoRI and XmnI. A probe containing the exon 4 sequence of ANT3 was used. (D) Semiquantitative RT-PCR was performed using the total RNA from WT and ANT3^{mut} cells to determine the mRNA levels of ANT1, ANT2, and ANT3. GAPDH was used as control. An ethidium bromide stain is shown. (E) siRNA of ANT2 or ANT3 was used to treat WT and ANT3^{mut} cells for 3 d, and the ANT3 or ANT2 protein levels were analyzed by WB using anti-ANT antibody. (F) ANT3^{mut} cells were infected with a lentivirus encoding GFP or ANT3, and the resulting cells were designated as ANT3^{mut}+GFP or ANT3^{mut}+ANT3, respectively. Thirty-six hours after infection, these cells were treated with TNF-α (50 ng/ml) for different periods of time, and cell survival rates were measured by PI exclusion. ANT3 mRNA levels in these cells were determined by semiquantitative RT-PCR. The ectopic expression of ANT3 was confirmed by Western blotting with anti-ANT antibody. (G) WT cells were infected with lentiviruses encoding siRNA targeting ANT3 or a control lentivirus. The resulting cells were designated as siANT3 or siVector, respectively. Forty-eight hours after infection, these cells were treated with TNF-α (50 ng/ml) for different periods of time, and the cell survival rates were measured. ANT3 mRNA levels in these cells were determined by semiquantitative RT-PCR. (H) The same as E except siANT2 was used. Comparable results were obtained in 2–5 independent experiments. The representative data are shown.

downstream of the stop codon. Figure 1C shows a Southern blot analysis of the *ANT3* gene disruption in ANT3^{mut} cells. A probe containing the exon 4 sequence of ANT3 detected a bigger fragment in EcoRI+XmnI-digested genomic DNA, indicating that one allele of *ANT3* contains a DNA insertion. We described in our previous report that our specially designed retroviral vector contains a self-cleavage ribozyme sequence that would diminish gene expression by cleavage the fused mRNA if the insertion occurred within the 3′ untranslated region (Zarubin *et al.,* 2005). Semiquantitative PCR (Figure 1D) and real-time PCR (data not shown) confirmed the reduction of ANT3 mRNA in ANT3^{mut} cells, suggesting that a functional ANT3 allele was indeed disrupted. We analyzed the other two ANT family members in wild-type and ANT3^{mut} cells and found that ANT1 mRNA is undetectable in MCF-7 cells, and ANT2 mRNA is slightly higher in ANT3^{mut} cells (Figure 1D). We have obtained an anti-ANT antibody, which detects all forms of ANT. WB analysis of the lysates from wild-type and ANT3^{mut} cells with anti-ANT antibody did not reveal a difference between these two cells (data not shown). Because ANT2 and ANT3 are not distinguishable in molecular weight, we believe this result reflects no significant difference of the total ANT proteins between wild-type and ANT3^{mut} cells.

To compare the level of ANT2 and ANT3 proteins between ANT3^{mut} and wild-type cells, we used small interfering RNA (siRNA) to knockdown ANT3 and ANT2, respectively, and then performed WB analysis using anti-ANT antibody. As shown in Figure 1E, we were able to detect increased ANT2 protein and decreased ANT3 protein in ANT3^{mut} cells. To determine that the reduction of ANT3 is responsible for TNF-resistance, we needed to reconstitute ANT3 expression in ANT3^{mut} cells. Lentiviruses can deliver genes into MCF-7 cells with almost 100% efficiency (data not shown), and therefore were used to express ANT3 in ANT3^{mut} cells. Lentivirus-mediated expression of ANT3 and green fluorescent protein (GFP) in ANT^{mut} cells did not affect the viability of the cells in a 3-d period (data not shown). The expression of ANT3 in ANT3^{mut} cells was confirmed by semiquantitative PCR and WB analysis with anti-ANT antibody (Figure 1F). Expression of ANT3, but not GFP, increased TNF-α–induced cell death in ANT3^{mut} cells (Figure 1F), indicating that the resistance to TNF-α–induced cell death in ANT3^{mut} cells is due to low ANT3 levels. To further confirm that ANT3 is involved in the TNF-α–induced death of MCF-7 cells, we knocked down ANT3 in wild-type MCF-7 cells and determined whether inhibition of ANT3 expression by siRNA affected TNF-α–induced cell death. As shown in Figure 1G, ANT3 expression was reduced by siRNA and the reduction of ANT3 expression led to a resistance to TNF-α–induced killing. To determine whether another ANT family member, ANT2, is involved in TNF-α–induced MCF-7 cell death, we knocked down ANT2 in MCF-7 cells by siRNA. We did not find significant difference between ANT2 knockdown cells and control cells with respect to TNF-α–induced cell death (Figure 1H). Therefore, ANT3 seems to be selectively involved in TNF-α–induced cell death in MCF-7 cells.

The ANT3^{mut} Line Is Resistant to Oxidative Stress–induced Cell Death

To establish whether ANT3^{mut} is selectively resistant to different death triggers, we examined its sensitivity to several death stimuli. In comparison with wild-type MCF-7 cells, ANT3^{mut} cells are 1) resistant to cell death induced by H_2O_2 and by the superoxide anion producer DQ (Farrington *et al.,* 1973; Figure 2, A and B). 2) They are moderately resistant to cell death induced by glucose starvation and by the microtubule disruptor vincristine (Figure 2, C and D). 3) They are almost equally sensitive to cell death induced by the alkylating agent mitomycin, the pyrimidine analogue 5-fluorouracil, the mitochondrial ATPase inhibitor oligomycin, and the K^+ ionophore valinomycin (Figure 2, E, F, G, and H). Restoring ANT3 expression in ANT3^{mut} cells increased TNF-, H_2O_2-, and glucose starvation–induced cell death (Figure 2I), which confirmed the role of ANT3. Because of the role of ANT in transporting ADP from the cytosol into mitochondria for ATP synthesis, it is worthwhile to note that oligomycin, which inhibits electron transport in mitochondria, and valinomycin, which induces a loss in the inner mitochondrial membrane potential, both induce similar levels of cell death in ANT3^{mut} and wild-type MCF-7 cells. Because ROS is involved in TNF-α–induced apoptosis, the data in Figure 2 suggest that ANT3 participates in the death process mediated and/or triggered by free radicals.

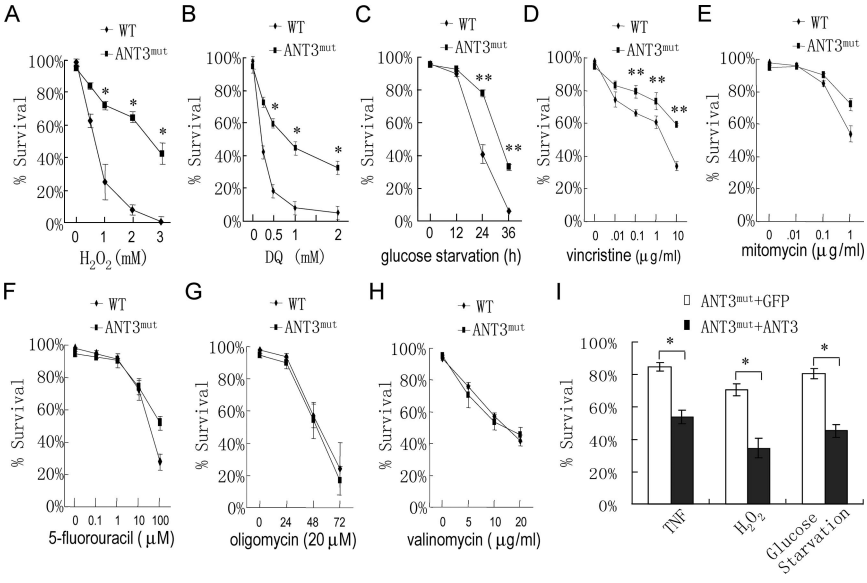

Figure 2. ANT3^{mut} MCF-7 cells are resistant to oxidative stress–induced cell death. WT and ANT3^{mut} cells were either treated with different concentrations of H_2O_2 (A), DQ (B), vincristine (D), mitomycin (E), 5-fluorouracil (F), or valinomycin (H) for 18, 24, 96, 96, 96, and 72 h, respectively, or they were incubated with glucose-free medium (C) or 20 μM oligomycin (G) for different periods of time. Cell survival rates were measured by PI exclusion. (I) ANT3^{mut} cells were infected with a lentivirus encoding GFP or ANT3. Thirty-six hours after infection, these cells were treated with TNF-α (50 ng/ml), H_2O_2 (1 mM), or glucose starvation for 24 h, and cell survival rates were measured by PI exclusion. *$p < 0.005$, **$p < 0.05$ (Student's t test). Data are the mean ± SD of triplicate samples.

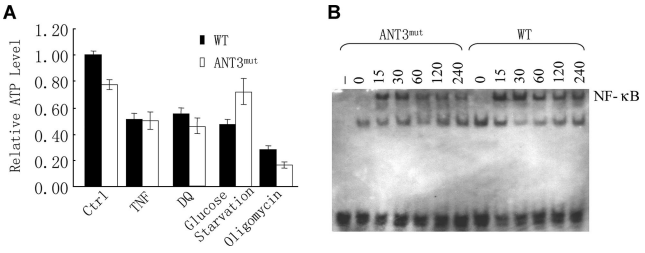

Figure 3. ANT3 mutation–mediated death resistance is not related to cellular ATP levels or the NF-κB pathway. (A) WT and ANT3^{mut} cells were left untreated (Ctrl) or were treated with TNF-α (50 ng/ml), DQ (0.5 mM), glucose starvation, or oligomycin (10 μM) for 12, 12, 9, and 9 h, respectively. Cells were collected and relative ATP levels were determined using the Enliten ATP assay kit (Promega). (B) WT and ANT3^{mut} cells were treated with TNF-α (50 ng/ml) for different periods of time. NF-κB activity was measured by EMSA. Comparable results were obtained in three independent experiments. The representative data are shown.

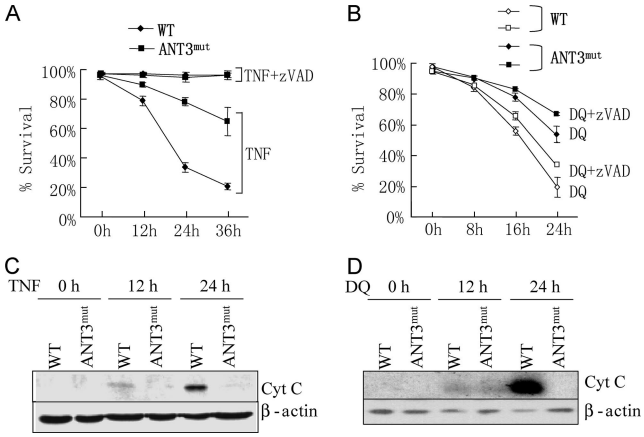

Figure 4. ANT3^{mut} cells have impaired cyt c release in apoptosis. (A) WT and ANT3^{mut} cells were treated with TNF-α alone (50 ng/ml) or TNF-α (50 ng/ml) + zVAD (1 μM) for different periods of time. Cell survival rates were measured by PI exclusion. (B) WT and ANT^{mut} cells were treated with DQ (0.5 mM) alone or DQ (0.5 mM) + zVAD (1 μM) for different periods of time. Cell survival rates were measured by PI exclusion. (C) WT and ANT3^{mut} cells were treated with TNF-α (50 ng/ml) for different periods of time. Cells were collected and subjected to fractionation. cyt c levels in the cytosol fraction were analyzed by Western blotting. β-actin levels were measured as a loading control. (D) WT and ANT3^{mut} cells were treated with DQ (0.5 mM) for different periods of time. Cells were subjected to analysis of cyt c release as in C. Comparable results were obtained in 2–3 independent experiments. The representative data are shown.

The Resistance of ANT3^{mut} Cells to Cell Death Is Not Related to Intracellular ATP Levels

Because of the role of ANT in ATP synthesis, we examined whether mutating ANT3 affected intracellular ATP levels and whether there is any correlation between intracellular ATP levels and cell death in wild-type and ANT3^{mut} MCF-7 cells. The ATP levels in ANT3^{mut} cells are ~80% of that found in wild-type cells (Figure 3A), indicating the ANT3 mutations do affect intracellular ATP levels. The mitochondria respiration chain inhibitor oligomycin was used as a control, which reduced ATP in both wild-type and ANT3^{mut} cell lines. TNF, DQ, and glucose starvation all reduced intracellular ATP levels to a certain extent in wild-type cells (Figure 3A), but the reduction levels do not correlate with their levels of induced cell death shown in Figures 1 and 2. Furthermore, when compared with wild-type MCF-7 cells, ANT3^{mut} cells had equal ATP levels after TNF treatment, slightly lower ATP levels after DQ treatment, and higher ATP levels after glucose starvation (Figure 3A). These observations indicate that ATP levels are not associated with ANT3 mutation–mediated resistance to TNF-, DQ-, or glucose starvation–induced cell death. Therefore, ANT3's function in ADP/ATP transport seems to be independent from its role in TNF-α–induced apoptosis.

ANT3 Deficiency Does Not Affect Survival Pathways

Cell death is determined by a balance between survival and death pathways. NF-κB is known to promote cell survival in many cell systems. Because TNF activates NF-κB in MCF-7 cells and because NF-κB was reported to be required for Akt overexpression– and dexamethasone-mediated inhibition of TNF-α–induced MCF-7 cell death (Burow *et al.*, 2000; Machuca *et al.*, 2006), we examined whether ANT3 mutation has any effect on TNF-α–induced NF-κB using an electromobility shift assay. We found that TNF-α–induced NF-κB activation is comparable in ANT3^{mut} and wild-type MCF-7 cells (Figure 3B). The PI3K-Akt pathway is another well-studied survival pathway, but its role in TNF-α–induced cell death is unclear. We found that the PI3K inhibitor LY294002 did not affect TNF-α–induced cell death in ANT3^{mut} or wild-type MCF-7 cells, and TNF did not induce any detectable change in Akt phosphorylation in either cell line as well (data not shown). Protein kinase C (PKC) seems to be a survival factor in TNF-α–treated MCF-7 cells, because its inhibitor bisindolylmaleimide enhances TNF-α–induced death (Basu *et al.*, 2001, 2002; Lu *et al.*, 2006). Treatment with this PKC inhibitor equally affected TNF-α–induced cell death in wild-type and ANT3^{mut} cells (data not shown), suggesting that ANT3 mutations do not affect the PKC pathway.

Cyt c Release in Apoptosis Is Impaired in ANT3^{mut} MCF-7 Cells

We next sought to determine the location of ANT3 in the TNF-α–induced apoptosis pathway. It is well established that TNF-α–induced apoptosis is initiated by caspase-8 activation. As expected, the inhibition of caspases by the pan caspase inhibitor zVAD blocked TNF-α–induced death in both wild-type and ANT3^{mut} MCF-7 cells (Figure 4A). Although TNF-α–induced cell death was significantly different between wild-type and ANT3^{mut} cells, zVAD treatment eliminated this difference by preventing apoptosis in both cells. This is consistent with the fact that ANT3 is a mitochondrial protein and that the mitochondria functions downstream of the initiator caspase in the apoptosis pathway. For a comparison, we also treated wild-type and ANT3^{mut} cells with DQ alone or together with zVAD and examined cell viability (Figure 4B). zVAD only slightly inhibited cell death in both wild-type and ANT3^{mut} cells, and the levels of cell death were still different between wild-type and ANT3^{mut} cells. Because MCF-7 cells lack caspase-3, a major execution caspase, the cell death pathway downstream of the mitochondria in MCF-7 cells is not very dependent on caspase (Janicke *et al.*, 1998). The modest effect of zVAD on DQ-induced cell death suggests that DQ-induced cell death is primarily effector caspases-independent. To confirm that ANT3 regulates mitochondrial events in apoptosis, we measured cyt c release from the mitochondria in TNF-α-treated wild-type and ANT3^{mut} cells. As with previ-

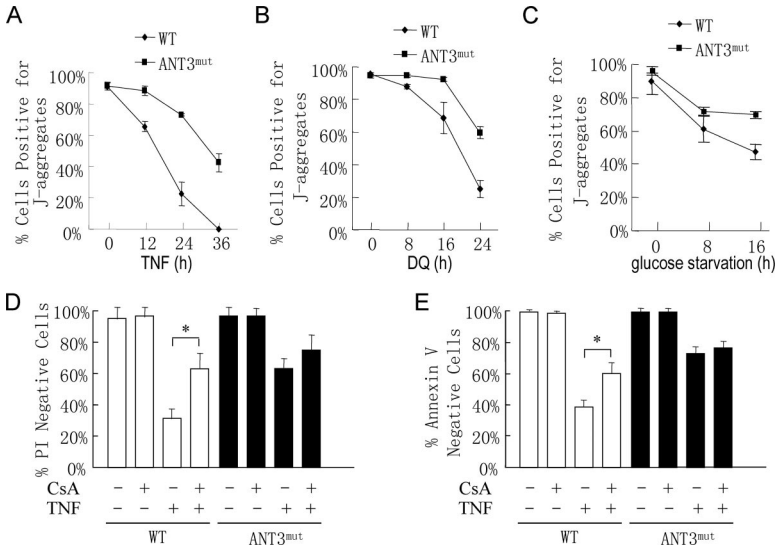

Figure 5. Comparison of $\Delta\psi_m$ changes and CsA's effect in WT and ANT3^{mut} cells. WT and ANT3^{mut} cells were treated with TNF-α (50 ng/ml; A) or DQ (0.5 mM; B) or were subjected to glucose starvation (C) for different periods of time. Cells were collected, and the mitochondria inner membrane potential ($\Delta\psi_m$) in live cells (PI-negative cells) was analyzed. J-aggregate–positive cells are those with normal $\Delta\psi_m$ values. Cell death was measured by PI exclusion (D) or annexin staining (E) in WT and ANT3^{mut} cells that were treated with or without TNF-α for 24 h in the presence or absence of 5 μM CsA. *$p < 0.01$ (Student's t test). Comparable results were obtained in two independent experiments. The representative data are shown.

ous reports, the release of cyt c into the cytosol was detected in TNF-α–treated wild-type MCF-7 cells (Figure 4C). We found that the TNF-α–induced release of cyt c was totally impaired in ANT3^{mut} cells (Figure 4C). Similarly, DQ-induced cyt c release was also totally impaired in ANT3^{mut} cells (Figure 4D). Collectively, these observations indicate that the function of ANT3 in TNF-α–induced but not DQ-induced apoptosis is controlled by signaling from an initiator caspase. Additionally, ANT3 is directly or indirectly involved in cyt c release in both TNF- and DQ-induced cell death in MCF-7 cells.

TNF-α–induced Mitochondrial $\Delta\psi_m$ Depolarization Is Attenuated in ANT3^{mut} Cells

Because $\Delta\psi_m$ depolarization is a key event in apoptosis, we sought to examine whether ANT3 participates in $\Delta\psi_m$ changes. $\Delta\psi_m$ was monitored using the fluorescent dye JC-1. JC-1 differentially stains mitochondria according to their $\Delta\psi_m$. Mitochondria with high $\Delta\psi_m$ accumulate red JC-1 aggregates, whereas mitochondria with low $\Delta\psi_m$ display the green monomeric form of JC-1. As expected, TNF treatment led to a decrease in J-aggregate fluorescence in live cells, indicating $\Delta\psi_m$ depolarization. The decrease in J-aggregate–positive cells in ANT3^{mut} cells was much slower than that in wild-type cells (Figure 5A), indicating that TNF-α–induced $\Delta\psi_m$ depolarization is attenuated by ANT3 mutation. Similarly, DQ- and glucose starvation–induced $\Delta\psi_m$ depolarization were also inhibited by ANT3 mutation (Figure 5, B and C). The $\Delta\psi_m$ depolarization (Figure 5) has some correlation with cell death (Figures 1 and 2), suggesting that effective $\Delta\psi_m$ depolarization and apoptosis require full function of ANT3.

To further evaluate the role of ANT3 in $\Delta\psi_m$ and cell death, we compared the effect of cyclosporin A (CsA), an mtPTP blocker, on TNF-α–induced cell death in wild-type and ANT3^{mut} cells. Both PI exclusion and annexin V staining were used to measure cell death. Inhibition of mtPTP reduced TNF-α–induced cell death in wild-type cells, but affected ANT3^{mut} cells very modestly (Figure 5, D and E). These data support the idea that ANT3 mutation affects mtPTP, and therefore ANT^{mut} cells are less affected by CsA in TNF-α–induced cell death.

Valinomycin is a K^+ ionophore that can disrupt $\Delta\psi_m$. At a concentration of 5 μg/ml, valinomycin does not cause significant cell death for up to 36 h in both wild-type and ANT3^{mut} MCF-7 cells (Figure 6A), but it is sufficient to induce $\Delta\psi_m$ depolarization (Figure 6B). As with its effect on cell death when higher doses or longer incubations were used (Figure 2H), valinomycin-induced $\Delta\psi_m$ depolarization is the same in wild-type and ANT3^{mut} cells (Figure 6B). In contrast, TNF-α–induced $\Delta\psi_m$ depolarization was much less in ANT3^{mut} cells (Figure 5A). When a treatment of TNF together with 5 μg/ml valinomycin was used, significant cell death occurred and no difference was found between

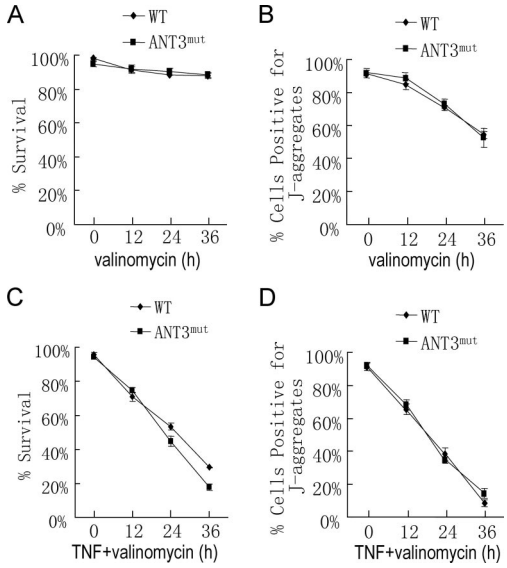

Figure 6. Disrupting $\Delta\psi_m$ by valinomycin overcomes the difference between WT and ANT3^{mut} cells with respect to TNF-α–induced cell death. (A) WT and ANT3^{mut} cells were treated with valinomycin (5 μg/ml) for different periods of time. Cell survival rates were measured by PI exclusion. (B) $\Delta\psi_m$ in cells described in A were analyzed as described in Figure 5. (C) WT and ANT3^{mut} cells were treated with TNF-α (50 ng/ml) together with valinomycin (5 μg/ml) for different periods of time. Cell survival rates were measured. (D) Percentages of J-aggregate–positive cells in cells described in C. Comparable results were obtained in two independent experiments. The representative data are shown.

wild-type and ANT3^{mut} cells (Figure 6C). Similarly, $\Delta\psi_m$ was lost in TNF+valinomycin–treated cells, and no differences were observed between wild-type and ANT3^{mut} cells. Valinomycin appears to be able to eliminate the difference between TNF-α–treated ANT3^{mut} and wild-type MCF-7 cells. These data support the idea that ANT3 mutation–mediated cell death resistance is related to its selective interference of TNF-α–induced $\Delta\psi_m$ depolarization.

ANT3 Mutation Alters TNF-α–induced ROS Response in MCF-7 Cells

Because free radical generation in the mitochondria has been implicated in $\Delta\psi_m$ depolarization in many cell systems, including TNF-α–induced apoptosis, we measured the redox state of TNF-α–treated ANT3^{mut} and wild-type cells using both HE and DCFH-DA. HE is often used to measure intracellular O_2^- because HE is oxidized to the fluorescent ethidium by O_2^-. DCFH-DA is widely used to measure H_2O_2 because cellular H_2O_2 is involved in generating fluorescent 2′-7′-dichlorofluorescein (DCF) from DCFH-DA via a multistep reaction. Both redox-measuring methods indicate that the ROS levels in ANT3^{mut} and wild-type cells were similar in a resting state (Figure 7A). However, the profiles of TNF-α–induced ROS in ANT3^{mut} and wild-type cells are different. TNF-induces a biphase ROS increase in wild-type cells, increasing at 1 h and falling back to background levels at 4 h before increasing again (Figure 7A). By contrast, TNF induced single-phase sustained ROS production in ANT3^{mut} cells (Figure 7A).

To check whether ANT3 mutation alters ROS responses in cases of other stimuli-induced cell death, we measured ROS in the cell death that ANT3 mutation was able to attenuate. ANT3^{mut} cells are resistant to H_2O_2- and DQ-induced cell death, but H_2O_2 and DQ interfere with ROS measurement, so they could not be used. ANT3 mutation also attenuates glucose starvation–induced cell death, though not as significantly as it does H_2O_2- or DQ-induced cell death. So we measured ROS in cells undergoing glucose starvation. As shown in Figure 7B, ROS levels in wild-type MCF-7 cells showed a biphase increase upon glucose starvation, and the ROS induction by glucose starvation in ANT3^{mut} cells is also sustained. To confirm that ANT3 deficiency is related to the change of ROS response in ANT3^{mut} cells, we knocked down ANT3 or overexpressed ANT3 in MCF-7 cells and then measured TNF-α–induced ROS. Knockdown of ANT3 in MCF-7 cells mimics the situation found in ANT^{mut} cells

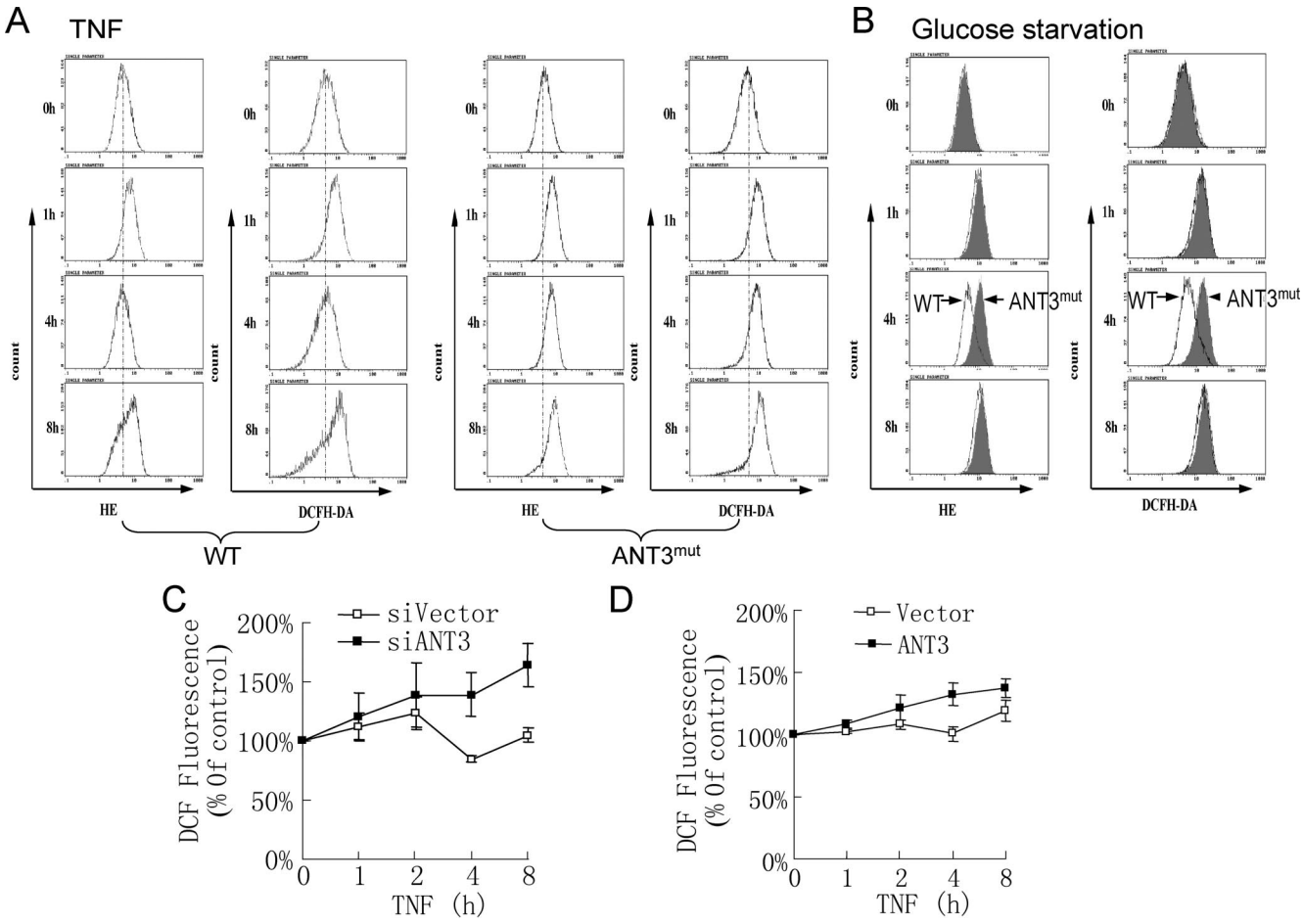

Figure 7. ANT3 mutation in MCF-7 cells alters TNF-α and glucose starvation–induced ROS production. (A) WT and ANT3^{mut} cells were treated with TNF-α (50 ng/ml) for different periods of time. Cells were collected, and live cells were gated for ROS analysis using HE or DCFH-DA. (B) WT and ANT3^{mut} cells were changed to glucose-free medium for different periods of time. ROS levels were analyzed as in A. (C) siANT3- or control vector-treated MCF-7 cells were stimulated with TNF-α for time periods as indicated. ROS levels in live cells were analyzed using DCFH-DA. (D) The same as C except ANT3 was ectopically expressed in MCF-7 cells before the analysis. Comparable results were obtained in 2–3 independent experiments. The representative data are shown.

(Figure 7C). Overexpression of ANT3 also disrupted the biphase ROS production and slightly increased ROS production (Figure 7D). Therefore, our data indicates that ANT3 is involved in the regulation of ROS levels, but the underlying mechanism is unclear.

DISCUSSION

Although ANTs are dispensable for TNF-α–induced death in hepatocytes (Kokoszka *et al.*, 2004), our genetic screen revealed that ANT3 is involved in TNF-α–induced MCF-7 cell death, suggesting that ANT participates in cell death in some systems. Cells with hypomorphic ANT3 expression are selectively resistant to some death stimuli, but not the others, which is consistent with the idea that ANT3 is dispensable for some types of cell death. A recent report that knockdown of ANT3 induces T-cell apoptosis (Jang and Lee, 2006) supports the involvement of ANT3 in cell death and further suggests that ANT3 can both positively and negatively influence cell death depending on cell systems. As with previously proposed models, ANT3 is indeed involved in the regulation of mtPTP in MCF-7 cells. This is evident by the observation that ANT3 mutation impaired the $\Delta\psi_m$ depolarization and subsequent release of cyt c from the mitochondria that normally follows exposure to TNF and other stimuli. Our study provides genetic evidence in support of the role of ANT3 in regulating mtPTP and cell death in some systems.

Although the role of mtPTP in cell death has been well established, gene knockout of cyclophilin D and ANT (Kokoszka *et al.*, 2004; Nakagawa *et al.*, 2005; Baines *et al.*, 2005), as well as our work describe herein, suggest there is significant complexity in this death control pore. Cyclophilin D is required for some necrotic, but not apoptotic, forms of cell death that were tested. ANT is not required for TNF- and Fas-induced hepatocyte death, but it is involved in TNF- and oxidative stress–induced MCF-7 cell death. Perhaps cyclophilin D and ANTs are regulatory components of mtPTP, and each of them senses different signals. If this is true, then the complexity also exists in the upstream signal pathway, because ANT's role in cell death is clearly cell type– and stimulus-dependent.

A number of studies suggest that oxidative stress is involved in TNF-α–induced cell death. Previous studies have shown that enhancing ROS production in TNF-α–treated MCF-7 cells by overexpressing NAD(P)H:quinone reductase or by treating the cells with vitamin D increases TNF-α–induced cell death (Siemankowski *et al.*, 2000; Weitsman *et al.*, 2003). However, TNF-α–induced ROS production in MCF-7 cells has not been extensively studied. We show that TNF induces biphase ROS production in MCF-7 cells. This biphase ROS production may relate to cell death because ANT3 mutation impairs the biphase ROS response to TNF stimulation. It needs to be noted that although many studies suggest that sustained ROS production causes damage, ANT3^{mut} cells, which have a sustained ROS increase upon TNF treatment or glucose starvation, have less cell death. Although we do not know the exact link between cell death and the pattern and levels of ROS in our system, our data suggests that TNF-α–induced apoptosis in MCF-7 cells is independent of the effect of ROS levels.

In vitro studies have shown that Ca^{2+} increases the generation of H_2O_2 by some unknown mechanism that is inhibited by CsA (Kanno *et al.*, 2004), a drug that binds to cyclophilin D, which in turn prevents cyclophilin D from binding to ANT and strongly inhibits mtPTP, suggesting that ANT is involved in ROS production. In the presence of inorganic phosphate, Ca^{2+} increases oxygen consumption and ROS production in isolated mitochondria, while decreasing the content of free thiols in ANT (Kanno *et al.*, 2004). We do not know if the role of ANT3 in the biphase ROS production is due to it counteracting ROS production or if it is targeted by ROS and thus decreases ROS in MCF-7 cells. It is hard to believe that more ROS in ANT3^{mut} cells leads to less cell death because it cannot be explained by current knowledge. Because of the possibility that ANT3 is a target of ROS, the ROS decrease observed in wild-type MCF-7 cells after 4 h of TNF treatment (Figure 7A) could be a result of the neutralization of ROS by ANT3. Therefore, it can be speculated that although ROS levels in wild-type cells were low at 4 h after TNF treatment, ANT3 had been damaged and MPT might have been induced. If this is true, we can also speculate that the loss of ANT3 might make the mtPTP insensitive to ROS so that even if TNF induced a sustained ROS elevation the cell death was still less.

Although cell death is associated with $\Delta\psi_m$ depolarization, the frequency of cell death in TNF-, DQ-, and valinomycin-treated cells does not precisely correlate with the level of $\Delta\psi_m$ depolarization. For example, TNF and DQ treatment resulted in similar cell death frequencies in MCF-7 cells (Figures 1A and 2B), but the percentage of cells positive for J-aggregates differs (Figure 5, A and B). In addition, 5 μg/ml valinomycin can effectively trigger $\Delta\psi_m$ depolarization, but its induced cell death is modest (Figure 6, A and B). Similarly, ROS is associated with cell death, but the level of ROS induction does not correlate well with cell death (Figure 7, A and B). The differences between ROS production in glucose-starved wild-type and ANT3^{mut} cells are bigger than that between TNF-α–treated wild-type and ANT3^{mut} cells, but ANT3^{mut} cells are less protected against glucose starvation than against TNF treatment. Therefore, an apoptotic process could be influenced by multiple factors in the mitochondria. It is clear that much more work is needed to understand how mtPTP is regulated. Our study presented here demonstrates that ANT3 is required for some apoptotic cell death. Our data supports the idea that the role of ANT3 in cell death is to regulate MPT.

ACKNOWLEDGMENTS

This work was supported in part by Grants NSFC30670442 and NSF30330260 and Grant NSFC-CIHR 30611120526 from Chinese National Science Foundation; Grants IRT0649 and J0630649 from Ministry of Education of China; and funds from Xiamen University.

REFERENCES

Baines, C. P. *et al.* (2005). Loss of cyclophilin D reveals a critical role for mitochondrial permeability transition in cell death. Nature *434*, 658–662.

Basu, A., Lu, D., Sun, B., Moor, A. N., Akkaraju, G. R., and Huang, J. (2002). Proteolytic activation of protein kinase C-epsilon by caspase-mediated processing and transduction of antiapoptotic signals. J. Biol. Chem. *277*, 41850–41856.

Basu, A., Mohanty, S., and Sun, B. (2001). Differential sensitivity of breast cancer cells to tumor necrosis factor-alpha: involvement of protein kinase C. Biochem. Biophys. Res. Commun. *280*, 883–891.

Bauer, M. K., Schubert, A., Rocks, O., and Grimm, S. (1999). Adenine nucleotide translocase-1, a component of the permeability transition pore, can dominantly induce apoptosis. J. Cell Biol. *147*, 1493–1502.

Burow, M. E., Weldon, C. B., Melnik, L. I., Duong, B. N., Collins-Burow, B. M., Beckman, B. S., and McLachlan, J. A. (2000). PI3-K/AKT regulation of NF-kappaB signaling events in suppression of TNF-induced apoptosis. Biochem. Biophys. Res. Commun. *271*, 342–345.

da Silva, C. J., Miranda, Y., Austin-Brown, N., Hsu, J., Mathison, J., Xiang, R., Zhou, H., Li, Q., Han, J., and Ulevitch, R. J. (2006). Nod1-dependent control of tumor growth. Proc. Natl. Acad. Sci. USA *103*, 1840–1845.

Dolce, V., Scarcia, P., Iacopetta, D., and Palmieri, F. (2005). A fourth ADP/ATP carrier isoform in man: identification, bacterial expression, functional characterization and tissue distribution. FEBS Lett. *579*, 633–637.

Farrington, J. A., Ebert, M., Land, E. J., and Fletcher, K. (1973). Bipyridylium quaternary salts and related compounds. V. Pulse radiolysis studies of the reaction of paraquat radical with oxygen. Implications for the mode of action of bipyridyl herbicides. Biochim. Biophys. Acta *314*, 372–381.

Ferguson, H. A., Marietta, P. M., and Van Den Berg, C. L. (2003). UV-induced apoptosis is mediated independent of caspase-9 in MCF-7 cells: a model for cytochrome c resistance. J. Biol. Chem. *278*, 45793–45800.

Goldstein, J. C., Waterhouse, N. J., Juin, P., Evan, G. I., and Green, D. R. (2000). The coordinate release of cytochrome c during apoptosis is rapid, complete and kinetically invariant. Nat. Cell Biol. *2*, 156–162.

Goossens, V., Grooten, J., De Vos, K., and Fiers, W. (1995). Direct evidence for tumor necrosis factor-induced mitochondrial reactive oxygen intermediates and their involvement in cytotoxicity. Proc. Natl. Acad. Sci. USA *92*, 8115–8119.

Jang, J.-Y., and Lee C.-E. (2006). IL-4-induced upregulation of adenine nucleotide translocase 3 and its role in Th cell survival from apoptosis. Cell. Immunol. *241*, 14–25.

Janicke, R. U., Sprengart, M. L., Wati, M. R., and Porter, A. G. (1998). Caspase-3 is required for DNA fragmentation and morphological changes associated with apoptosis. J. Biol. Chem. *273*, 9357–9360.

Kanno, T., Sato, E. E., Muranaka, S., Fujita, H., Fujiwara, T., Utsumi, T., Inoue, M., and Utsumi, K. (2004). Oxidative stress underlies the mechanism for Ca(2+)-induced permeability transition of mitochondria. Free Radic. Res. *38*, 27–35.

Kokoszka, J. E., Waymire, K. G., Levy, S. E., Sligh, J. E., Cai, J., Jones, D. P., MacGregor, G. R., and Wallace, D. C. (2004). The ADP/ATP translocator is not essential for the mitochondrial permeability transition pore. Nature *427*, 461–465.

Kroemer, G. and Reed, J. C. (2000). Mitochondrial control of cell death. Nat. Med. *6*, 513–519.

Lu, D., Huang, J., and Basu, A. (2006). Protein kinase Cepsilon activates protein kinase B/Akt via DNA-PK to protect against tumor necrosis factor-alpha-induced cell death. J. Biol. Chem. *281*, 22799–22807.

Machuca, C., Mendoza-Milla, C., Cordova, E., Mejia, S., Covarrubias, L., Ventura, J., and Zentella, A. (2006). Dexamethasone protection from TNF-alpha-induced cell death in MCF-7 cells requires NF-kappaB and is independent from AKT. BMC Cell Biol. *7*, 9.

Marzo, I. *et al.* (1998). Bax and adenine nucleotide translocator cooperate in the mitochondrial control of apoptosis. Science *281*, 2027–2031.

Nakagawa, T., Shimizu, S., Watanabe, T., Yamaguchi, O., Otsu, K., Yamagata, H., Inohara, H., Kubo, T., and Tsujimoto, Y. (2005). Cyclophilin D-dependent mitochondrial permeability transition regulates some necrotic but not apoptotic cell death. Nature *434*, 652–658.

Ono, K., Wang, X., and Han, J. (2001). Resistance to tumor necrosis factor-induced cell death mediated by PMCA4 deficiency. Mol. Cell. Biol. *21*, 8276–8288.

Pastorino, J. G., Simbula, G., Yamamoto, K., Glascott, P. A., Jr., Rothman, R. J., and Farber, J. L. (1996). The cytotoxicity of tumor necrosis factor depends on induction of the mitochondrial permeability transition. J. Biol. Chem. *271*, 29792–29798.

Siemankowski, L. M., Morreale, J., Butts, B. D., and Briehl, M. M. (2000). Increased tumor necrosis factor-alpha sensitivity of MCF-7 cells transfected with NAD(P)H:quinone reductase. Cancer Res. *60*, 3638–3644.

Stepien, G., Torroni, A., Chung, A. B., Hodge, J. A., and Wallace, D. C. (1992). Differential expression of adenine nucleotide translocator isoforms in mammalian tissues and during muscle cell differentiation. J. Biol. Chem. *267*, 14592–14597.

Strasser, A., O'Connor, L., and Dixit, V. M. (2000). Apoptosis signaling. Annu. Rev. Biochem. *69*, 217–245.

Temkin, V., Huang, Q., Liu, H., Osada, H., and Pope, R. M. (2006). Inhibition of ADP/ATP exchange in receptor-interacting protein-mediated necrosis. Mol. Cell. Biol. *26*, 2215–2225.

Wang, X., Ono, K., Kim, S. O., Kravchenko, V., Lin, S. C., and Han, J. (2001). Metaxin is required for tumor necrosis factor-induced cell death. EMBO Rep. *2*, 628–633.

Weitsman, G. E., Ravid, A., Liberman, U. A., and Koren, R. (2003). Vitamin D enhances caspase-dependent and independent TNF-induced breast cancer cell death: the role of reactive oxygen species. Ann. NY Acad. Sci. *1010*, 437–440.

Zamora, M., Granell, M., Mampel, T., and Vinas, O. (2004). Adenine nucleotide translocase 3 (ANT3) overexpression induces apoptosis in cultured cells. FEBS Lett. *563*, 155–160.

Zamzami, N. and Kroemer, G. (2001). The mitochondrion in apoptosis: how Pandora's box opens. Nat. Rev. Mol. Cell Biol. *2*, 67–71.

Zarubin, T., Jing, Q., New, L., and Han, J. (2005). Identification of eight genes that are potentially involved in tamoxifen sensitivity in breast cancer cells. Cell Res. *15*, 439–446.